Deep Learning-Assisted Demodulation for TeraHertz Communications Under Hybrid Distortions

Dongxuan He and Zhaocheng Wang, *Fellow, IEEE*

***Abstract*— TeraHertz wireless communication has been regarded as an effective technology to satisfy the ever-increasing requirements of high-rate services, where the imperfections of TeraHertz devices, including in-phase/quadrature imbalance, phase noise and nonlinearity, regarded as hybrid distortions, have to be investigated. Due to the hybrid distortions, the explicit system model could not be mathematically derived, which limits the performance of the state-of-the-art demodulation methods. Here, a deep learning-assisted demodulation methodology is proposed to improve the bit error rate performance. Specifically, a multiple-output deep feedforward neural network is designed to fit the mapping between the received signal and likelihood information, where the number of outputs equals to the size of the modulation set, thus enabling the demodulation of the overlapped received signals corresponding to different constellation points. Besides, a training set generation method is proposed to generate the training examples without the prior knowledge of likelihood information. Simulation results validate that the proposed learning-assisted methodology could improve the demodulation performance of the TeraHertz wireless systems under severe hybrid distortions.**

***Index Terms*— TeraHertz wireless communication, hybrid distortion, signal demodulation, deep feedforward neural network.**

I. Introduction

With the ever-increasing demand of ultra-high-rate wireless communications, TeraHertz (THz) communication (from 0.1 to 10 THz), which provides broad bandwidth at the order of tens or hundreds of GHz, has drawn much research attention [1]–[4]. In particular, THz communication is capable of realizing transmission throughput up to terabit-per-second (Tbps), which enables a plurality of services, including ultra-broadband wireless links, holographic video conferences, fiber extender, etc. Therefore, it has been regarded as a key technology for the upcoming sixth-generation (6G) mobile communications [5].

Manuscript received September 16, 2021; revised October 13, 2021 and November 6, 2021; accepted December 2, 2021. Date of publication December 6, 2021; date of current version February 12, 2022. This work was supported in part by the National Natural Science Foundation of China under Grant 62101306, in part by the National Key R&D Program of China under Grant 2018YFB1801501, in part by Shenzhen Special Projects for the Development of Strategic Emerging Industries (20180608143929064O), and in part by Shenzhen Wireless Over VLC Technology Engineering Lab Promotion. The associate editor coordinating the review of this letter and approving it for publication was V.-D. Nguyen. *(Corresponding author: Zhaocheng Wang.)*

Dongxuan He is with the Beijing National Research Center for Information Science and Technology, Department of Electronic Engineering, Tsinghua University, Beijing 100084, China (e-mail: dongxuan_he@mail.tsinghua.edu.cn).

Zhaocheng Wang is with the Beijing National Research Center for Information Science and Technology, Department of Electronic Engineering, Tsinghua University, Beijing 100084, China, and also with the Tsinghua Shenzhen International Graduate School, Shenzhen 518055, China (e-mail: zcwang@tsinghua.edu.cn).

Digital Object Identifier 10.1109/LCOMM.2021.3132965

Nevertheless, different from low frequency bands, THz signals suffer from high path loss, severe hybrid distortions, and significant combined noise[1] [1], [6]. Especially, when considering hardware costs and energy consumption in practical systems, THz transceiver usually employs cheap and energy-efficient radio frequency (RF) devices. The imperfections of those devices, which include the mixture of the in-phase/quadrature imbalance of RF branches, the nonlinearity of power amplifier, and the phase noise of local oscillator (LO), make the THz signals suffer from severe hybrid distortions [6], [7]. Moreover, such distortions could not be effectively handled by minimum mean squared error (MMSE) equalization, which aims to eliminate the influence of multi-path effects and inter-symbol interference. Although pre-distortion or compensation algorithms can mitigate the impact of such distortions [8], [9], high-rate and high-resolution RF links are required to collect the distorted signal and obtain the exact distortion characteristics, which is expensive for THz communication systems.

Meanwhile, deep learning, also known as deep neural network, has become an emerging technology to address intractable problems for various wireless communication scenarios, such as beamforming design, resource allocation, channel estimation, etc. [10]. The researchers have also developed specific deep neural networks to improve the performance of signal demodulation. For example, Zhang *et al.* [11] proposed a deep learning based receiver architecture to demodulate the real-world WiFi data. Honkala *et al.* [12] proposed a fully deep learning receiver structure to recover the received signal. Besides, Wang *et al.* [13] utilized the deep neural networks to indirectly extract features of received signals or directly detected the category of signals. Due to the hybrid distortions caused by THz transceiver, the received symbols corresponding to different constellation points might overlap under low signal-to-noise ratio (SNR). As a result, the demodulation performance of the conventional deep learning method, that is, single-output deep feedforward neural network (SoDFNN), which directly fits the mapping between the received symbol and the demodulation result, is limited. To tackle this problem, a multiple-output deep feedforward neural network (MoDFNN), which has the same number of outputs as the size of the modulation set, is proposed to demodulate the THz signals under severe hybrid distortions.

The main contributions of this letter are summarized as follows: 1) MoDFNN having the same number of outputs as the size of the modulation set is proposed to fit the

[1]TeraHertz signal suffers from a combined noise, which includes thermal noise, molecular absorption noise, quantum noise, etc.

mapping between the received THz symbol and the likelihood information; 2) A specific training example generation method is derived, whereby the training examples labeled with one-hot vector are utilized to train a deep neural network for outputting likelihood information while prior knowledge about the hybrid distortions is not known. Simulation results demonstrate that the superiority of our proposed MoDFNN in comparison to MMSE equalization, support vector machine (SVM)-based classification and the traditional deep learning method.

II. System Model

We consider an end-to-end THz communication system, where both transmitter and receiver are equipped with single Cassegrain antenna to provide sufficient antenna gain [3]. Without loss of generality, we adopt an equivalent baseband model, let $x = x_I + jx_Q$ be the complex-valued symbol to be transmitted, where x_I and x_Q are the corresponding signals of the in-phase (I) and quadrature (Q) branches. Furthermore, x is an element of modulation set χ, where $|\chi| = 2^M$ is the modulation order and M is the number of bits per symbol. Due to the imperfections of THz devices, the signal x will be distorted at both the transmitter and the receiver.

A. Distortion of THz Transmitter

Before transmission, the symbol x is up-converted to the desired carrier frequency. The mismatch between two RF branches makes the signal suffer from I/Q imbalance, and the effect of the voltage-controlled oscillator (VCO) makes the signal suffer from phase noise.[2] Therefore, the transmitted signal will be distorted, which can be modeled as

$$\widetilde{x} = (\mu_T x + v_T x^*)\, e^{j\theta_T}, \tag{1}$$

where $()^*$ denotes the complex conjugation operation, θ_T is the phase noise. μ_T and v_T are the imbalance-related parameters at the transmitter, given by [6], [7], [9]

$$\mu_T = \cos(\phi_T) - j\varepsilon_T \sin(\phi_T), \tag{2}$$

$$v_T = \varepsilon_T \cos(\phi_T) - j\sin(\phi_T), \tag{3}$$

where ε_T and ϕ_T are the amplitude imbalance and phase imbalance between I and Q branches, respectively.

When up-converted to the desired frequency, the signal is then amplified by the power amplifier. Due to the nonlinearity of the power amplifier, the signal suffers from nonlinear distortion, which includes both amplitude compression and phase rotation. To describe the features of the amplifier, we adopt odd order memoryless polynomial model to relate the samples of input and output signals of the amplifier [7]. As such, the output samples of the amplifier are given as a function of the input samples, which can be formulated as

$$\tilde{s} = \sum_{k=1}^{K} \alpha_{2k-1} \widetilde{x} |\widetilde{x}|^{2(k-1)}, \tag{4}$$

where $2K-1$ is the order of nonlinearity, α_{2k-1} are the complex model parameters, and $|\cdot|$ represents the absolute value of a complex scalar.[3]

[2]For a typical VCO, the phase noise increases with the square of the center frequency. As such, the phase noise for a THz system cannot be ignored.

[3]In particular, we assume that the power amplifier works away from saturation region to guarantee the reliable performance, which can be realized be an appropriate back-off [7].

B. Distortion of THz Receiver

The amplified signal is then received after transmitting through the THz channel, where the received symbol can be expressed as

$$r = h\tilde{s} + w, \tag{5}$$

where $h = PL \cdot e^{j\kappa}$ denotes the channel response, and w denotes the baseband-equivalent Gaussian noise with noise power spectral density of N_0^2. Here, PL denotes the path loss, including the impact of antenna misalignment, frequency dependent loss, and frequency dispersion index, κ denotes the phase shift. Due to the imbalance of RF branches and the phase noise of the VCO at the receiver, the received signal r is further distorted, and the similar expression is adopted to model such distortions, which can be expressed as

$$\widetilde{r} = (\mu_R r + v_R r^*)\, e^{j\theta_R}, \tag{6}$$

where θ_R is the phase noise, μ_R and v_R are the distortion-related parameters, given by

$$\mu_R = \cos(\phi_R) - j\varepsilon_R \sin(\phi_R), \tag{7}$$

$$v_R = \varepsilon_R \cos(\phi_R) - j\sin(\phi_R), \tag{8}$$

where ε_R and ϕ_R are the amplitude imbalance and phase imbalance between I and Q branches at the receiver, respectively.

C. Problem Formulation

When the distorted received symbol $\widetilde{r}$ is obtained, for the conventional soft demodulation methods, it is demodulated according to the likelihood function $\Lambda(\widetilde{r}|s_m)$, for example, the decision of the optimal maximum likelihood detector can be expressed as

$$m^* = \underset{m=0,\cdots,2^M-1}{\arg\max}\ \Lambda(\widetilde{r}|s_m), \tag{9}$$

where s_m is the m-th transmit symbol of χ.

Due to the hybrid distortions caused by the imperfections of TeraHertz devices, the THz signals cannot be easily handled by the MMSE method since the expression of $\widetilde{r}$ is complicated. Moreover, an exact $\Lambda(\widetilde{r}|s_m)$ is difficult to be obtained without any prior knowledge about the distortions parameters. Thus, (9) can not be solved by the conventional methods directly.[4] To tackle this problem, we propose a deep learning-assisted demodulation methodology that is capable of solving (9) effectively under severe hybrid distortions.

III. Proposed Deep Learning-Assisted Demodulation Methodology

In this section, our proposed deep learning-assisted demodulation methodology is detailed. Specifically, a multiple-output deep feedforward neural network is proposed to fit the nonlinear mapping between the received symbol $\widetilde{r}$ and the demodulation likelihood information vector $\mathbf{P} = [p_0, \cdots, p_{2^M-1}]$, where each element of $\mathbf{P}$ can be expressed as

$$p_m = \Lambda(\widetilde{r}|s_m). \tag{10}$$

[4]The classical regression method can not estimate coefficient to an uncertain problem without explicit expression. Besides, classification methods, such as support vector machine (SVM), can not provide likelihood information for further processing such as decoding.

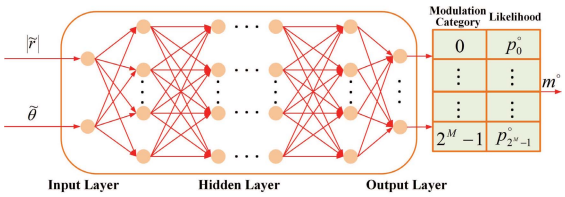

Fig. 1. The structure of our proposed deep learning-assisted demodulation.

Due to the outstanding fitting ability of DFNN, it is appropriate to utilize DFNN to learn the nonlinear mapping between $\widetilde{r}$ and $\mathbf{P}$.[5] Moreover, the detailed expression of the mapping between $\widetilde{r}$ and $\mathbf{P}$ is not required during the construction of DFNN.

A. Multiple-Output Deep Feedforward Neural Network

The structure of the proposed deep learning-assisted demodulation is shown in Fig.1, which consists of a cascade of three layers, i.e., the input layer, hidden layer, and output layer. In particular, the amplitude information $|\widetilde{r}|$ and phase information $\widetilde{\theta}$ are selected as the inputs of DFNN, where $\widetilde{r} = |\widetilde{r}|e^{j\widetilde{\theta}}$. Besides, the dimension of the output layer of our proposed demodulation structure is determined by the size of modulation set, where $L_o = 2^M$.

To be noticed, some works proposed to utilize a SoDFNN to realize the demodulation, but its performance is limited under low SNR [15]. While our proposed demodulation with multiple-output deep feedforward neural network could improve the demodulation accuracy and robustness significantly even under low SNR. The main reason for the performance gain is that the received symbols corresponding to different constellation points could overlap under low SNR, which affects the training of SoDFNN but not the training of MoDFNN.

We note that there are multiple layers in the hidden layer for a typical DFNN and all the layers are fully connected, where the output of one layer is the input of its subsequent layer. To this end, the output of the i-th layer can be formulated as

$$\mathbf{x}_i = f\left(\mathbf{W}_i\mathbf{x}_{i-1} + \mathbf{b}_i\right), \tag{11}$$

where $\mathbf{W}_i$ and $\mathbf{b}_i$ denote the weight matrix and bias of the i-th layer, respectively, $f(\cdot)$ denotes the activation function. Specifically, identity function is selected as the activation function of the output layer, given by $f(x) = x$, and Sigmoid function is selected as the activation function of the hidden layer to introduce nonlinearity, given by $f(x) = \frac{1}{1+e^{-x}}$.

Assuming a DFNN with L_h hidden layers is adopted to demodulate the received signal, the parameter matrix of the network can be expressed as $\mathbf{W} = [\mathbf{W}_1, \mathbf{b}_1, \cdots, \mathbf{W}_{L_h}, \mathbf{b}_{L_h}]$. As mentioned previously, the well-trained DFNN is capable of fitting the nonlinear mapping between the received symbol and the demodulation likelihood information, which can be formulated as

$$\mathbf{P}^\circ = \left[p_0^\circ, \cdots, p_{2^M-1}^\circ\right] = g\left(|\widetilde{r}|, \widetilde{\theta}; \mathbf{W}\right). \tag{12}$$

To optimize the performance of learning-assisted demodulation, the target of our proposed multiple-output DFNN is to train $\mathbf{W}$ such that $\mathbf{P}^\circ$ approaches $\mathbf{P}$. Therefore, mean squared error (MSE) is adopted as the learning performance metric, and the well-trained DFNN should satisfy

$$J(\mathbf{W}) = \mathbb{E}_{\widetilde{r}}\left(|\mathbf{P} - \mathbf{P}^\circ|^2\right) \le \epsilon, \tag{13}$$

where ϵ is the target training error.

B. Training of Neural Network

We now detail how our DFNN can be trained to obtain the likelihood information vector $\mathbf{P}$ to demodulate the received symbol. Specifically, the training process of the DFNN is performed through two steps: 1) Generate the training set and 2) Use the generated training set to train the DFNN such that W satisfying (13) is obtained.

1) Training Set Generation: In this step, we generate the training set $\mathcal{S}$ consisting of L training examples. In particular, each training example should include the information of the received symbol and the corresponding likelihood information, given by $\mathcal{S}_l = \left\{\left(|\widetilde{r}_l|, \widetilde{\theta}_l\right) \to \mathbf{P}_l\right\}$, where $l = 1, \cdots, L$.

We note that the likelihood information for each received symbol $\widetilde{r}_l$ is difficult to obtain. Thus, a convenient training set generation method is proposed, where the likelihood information vector $\mathbf{P}_l$ can be replaced by $\widetilde{\mathbf{P}}_l$. Here, $\widetilde{\mathbf{P}}_l$ is a one-hot vector with 0 and 1. Specifically, the element corresponding to the position of the actual modulation category is 1, while all the other elements are 0, in detail, $\widetilde{\mathbf{P}}_l$ can be expressed as

$$\widetilde{\mathbf{P}}_l = \underbrace{[0, \cdots, 1, \cdots, 0]}_{\text{The } m\text{-th element is 1}}. \tag{14}$$

Based on the law of large number, $\mathbb{E}_{\widetilde{r}}\left(\widetilde{\mathbf{P}}_l\right)$ converges to $\mathbf{P}^o$ when L is large enough.[6] When the size of the training set is sufficiently large, the DFNN based on $\widetilde{\mathcal{S}}_l$ can achieve the same mapping as the DFNN based on $\mathcal{S}_l$, which validates the feasibility of replacing the training example $\mathcal{S}_l$ by $\widetilde{\mathcal{S}}_l = \left\{\left(|\widetilde{r}|_l, \widetilde{\theta}_l\right) \to \widetilde{\mathbf{P}}_l\right\}$.

Relying on the one-hot code labeled training example, the MoDFNN can be well trained to accurately fit the mapping between the received symbol and the likelihood information without any prior knowledge. Moreover, the one-hot code provides the prior knowledge about the modulation type during training, which could improve the demodulation performance.

2) Training of $\mathbf{W}$*:* In this step, the generated training set $\widetilde{\mathcal{S}} = \left\{\widetilde{\mathcal{S}}_1, \widetilde{\mathcal{S}}_2, \cdots, \widetilde{\mathcal{S}}_L\right\}$ is used to train the DFNN such that the weight matrix $\mathbf{W}$ satisfies the constraint in (13). When Levenberg-Marquardt method is used [16], which is suitable for training the neural network when the learning performance metric is the sum of squares of nonlinear functions, $\mathbf{W}$ in the $(n+1)$-th update can be expressed as

$$\mathbf{W}^{n+1} = \mathbf{W}^n - \frac{1}{2\mu_n}\nabla F\left(\mathbf{W}^n\right), \tag{15}$$

where μ_n is the training parameter and

$$\nabla F\left(\mathbf{W}^n\right) = 2\mathbf{J}\left(\mathbf{W}^n\right)\mathbf{e}\left(\mathbf{W}^n\right). \tag{16}$$

[5]DFNN can approximate any measurable function with any desired degree of accuracy [14].

[6]Benefited from ultra-high-rate THz communications, abundant training examples can be transmitted within a short time, which enables THz transceiver to experimentally find an appropriate size of the training sample set during initialization. For future research, it is worth investigating the theoretical method to determine the optimal size of training sample set.

In (16), $\mathbf{J}(\cdot)$ denotes the Jacobian matrix and $\mathbf{e}(\mathbf{W}^n) = \left[e_1(\mathbf{W}^n), e_2(\mathbf{W}^n), \cdots, e_L(\mathbf{W}^n)\right]$, where $e_l(\mathbf{W}^n) = |g(\widetilde{r}_l, \mathbf{W}^n) - \widetilde{\mathbf{P}}|$ for $l \in (1, \cdots, L)$.

We keep updating $\mathbf{W}$ until the training performance metric is optimized. Next, the well-trained multiple-output DFNN is utilized to demodulate the received symbol. For a new received symbol $\widetilde{r}$, we generate the symbol information $\left(|\widetilde{r}|, \widetilde{\theta}\right)$ and input it into the DFNN. The category of current received symbol is the one which achieves the largest likelihood information among all the outputs of the DFNN, given by

$$m^{\circ} = \underset{m=0,\cdots,2^M-1}{\arg\max}\ p_m^{\circ}. \tag{17}$$

To estimate the parameters of MoDFNN, the training complexity is about $\mathcal{O}(N_{\text{DFNN}}^2)$ with N_{DFNN} denoting the total number of adaptive parameters [17]. Given a well-trained MoDFNN, the computational complexity is relatively low, since a well-trained MoDFNN can obtain the required likelihood information with only finite steps of calculation, and realize a satisfying demodulation performance.

Moreover, regardless of the number of antennas at transmitter and receiver, the mapping between the received symbol and the likelihood information can always be obtained by MoDFNN. Therefore, our proposed MoDFNN can work efficiently even in multi-input multi-output (MIMO) systems.

IV. Simulation Results

In this section, we present the simulation results to verify the effectiveness of our proposed deep learning-assisted signal demodulation methodology for THz communication under hybrid distortions. In particular, the THz transceiver works at 220 GHz and the transmission distance is 10m, hence the path loss is about 100dB [1]. Benefit from the directionality of Cassegrain antennas, a single-path THz channel is considered, where the transmit and receive antenna gains both are 20dBi [19]. The phase noise follows a block walk model which will change once per transmission block.[7] Especially, the phase noise can be expressed as $\theta_{t+1} = \theta_t + \Delta\theta_t$, where θ_t is the phase noise of the t-th block and $\Delta\theta_t$ is the change of phase noise between adjacent blocks, which is a Gaussian random variable with $\Delta\theta_t \sim N\left(0, (5^{\circ})^2\right)$. Other distortion parameters are also provided, where $\varepsilon_T = 0.3$, $\varepsilon_R = 0.2$, $\phi_T = \phi_R = 2^{\circ}$, and the order of nonlinearity of the amplifier is $(2K-1) = 5$ with $\alpha_1 = 1.0108 + j0.0858$, $\alpha_3 = 0.0879 - j0.1583$, and $\alpha_5 = -1.099 - j0.8991$. To assess the performance, $L_t = 10^3$ transmission blocks are generated, where the length of each block is 16200.

The demodulation schemes are detailed as follows

1) MMSE: The demodulation scheme with linear MMSE equalizer, where frequency domain MMSE equalization is executed before data demodulation.[8] Particularly, $L_{\text{MMSE}} = 10^4$ symbols are utilized to estimate the channel, and the FFT size of MMSE algorithm is N_{FFT}=1024.
2) SVM: The classification based demodulation, where SVM is used to determine the category of the received symbol directly [21]. The training length is $L_{\text{SVM}} = 10^4$.
3) SoDFNN: The learning-assisted demodulation with single-output DFNN, where the DFNN outputs the modulation category of the received symbol directly. Specifically, a SoDFNN with $L_h = 4$ is considered, where the number of neurons in the hidden layer are $(10, 10, 10, 10)$.
4) MoDFNN: Our proposed learning-assisted demodulation with multiple-output DFNN, as described in Section III.

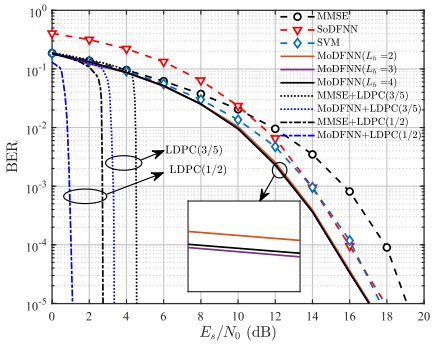

Fig. 2. Performance comparison of MMSE, SoDFNN, and our proposed MoDFNN with QPSK modulation.

In Fig. 2, we plot the BER versus E_s/N_0 for different schemes, where E_s is the average energy per symbol. For both SoDFNN and MoDFNN schemes, we use $L = 10^4$ training examples, generated by the system model described in Section II, to train the DFNNs. It is clear that the BER performance of the MMSE scheme degrades significantly, indicating that MMSE equalization cannot efficiently mitigate the hybrid distortions caused by imperfections of THz devices. The performance of the SoDFNN scheme becomes firstly worse and then better than the MMSE scheme, since the training of a single-output DFNN needs deterministic training examples, which are not strictly separated when SNR is relatively low. The performance of SVM is better than SoDFNN when SNR is relatively low, and tends to be the same as SoDFNN when SNR becomes high. This is because the kernel function of SVM can map the non-separable data into high-dimensional separable space. Specifically, our proposed MoDFNN has around 1.5 dB performance gain when compared to SoDFNN and 0.5 dB performance gain when compared to SVM at the BER of 10^{-2}.

In addition, the impact of the depth of the hidden layer (denoted by L_h) on the performance of our proposed MoDFNN is evaluated, where three MoDFNNs with $L_h = 2$, 3, and 4 are considered, respectively. The number of neurons in the hidden layers of these DFNNs is (10, 10), (10, 10, 10), and (10, 10, 10, 10), respectively. From Fig. 2, it is apparent that the proposed MoDFNN with $L_h = 3$ achieves the best performance, while the performance of DFNNs with $L_h = 2$ and 4 are slightly degraded because of underfitting and overfitting, which indicates that the performance of our proposed methodology is determined by the selection of the hyperparameters of the neural networks.

[7]Random-walk model is commonly utilized to describe strong phase noise, whereby the phase noise varies per transmission due to the ultra-high rate of THz communication [18].

[8]The frequency domain MMSE equalization is adopted to suppress the harmonic components caused by the nonlinearity of amplifier and recover the phase shift caused by phase noise. The computational complexity of MMSE is $\mathcal{O}(3N_{\text{MMSE}}+1)$ with N_{MMSE} denoting the total number of adaptive parameters [20]. Given a well-trained MMSE equalizer, only finite steps of calculation is required.

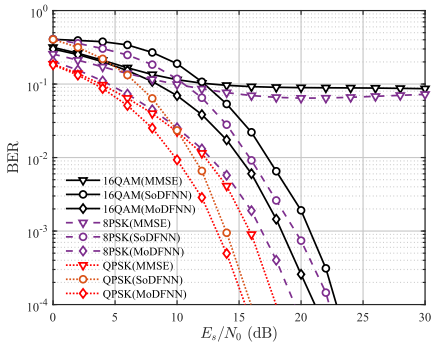

Fig. 3. Performance comparison of MMSE, SoDFNN, and our proposed MoDFNN with various modulations.

Furthermore, the BER performances of low-density parity check (LDPC) are presented to verify the effectiveness of our proposed scheme when soft-decision demodulation is considered.[9] It can be observed that, since MoDFNN can obtain accurate likelihood information under severe hybrid distortions, our proposed MoDFNN has around 1.5 dB performance gain with code rate $1/2$ and 1 dB performance gain with code rate $3/5$ when compared to MMSE at the BER of 10^{-5}.

In Fig. 3, BER performances of MMSE, SoDFNN and our proposed MoDFNN with $L_h = 3$ for various modulations (including QPSK, 8PSK and 16QAM) are evaluated. It is observed that the BER performance deteriorates considerably as the modulation order increases, which indicates the adverse effects of hybrid distortions, especially when high order modulations are adopted. However, our proposed deep learning-assisted demodulation methodology could improve the BER performance significantly. For example, our proposed MoDFNN has a 3dB performance gain with 8PSK modulation and a 2dB performance gain with 16QAM, when compared to SoDFNN at the BER of 10^{-2}, which validates the effectiveness of our proposed MoDFNN for THz wireless communication under hybrid distortions.

Finally, we further examine the complexity of different schemes, where the number of required multiplications per symbol estimation for MMSE, SVM, SoDFNN and MoDFNN are $4\log_2(N_{\text{FFT}})+4$, $2^M(L_{\text{SVM}}+2)$, $2N_1+\sum_{i=1}^{L_h-1} N_iN_{i+1}+N_{L_h}$ and $2N_1+\sum_{i=1}^{L_h-1} N_iN_{i+1}+2^MN_{L_h}$, respectively, with N_i denoting the number of neurons in the i-th hidden layer of SoDFNN and MoDFNN. It is evident that both SoDFNN and MoDFNN have the similar calculation complexity.

V. Conclusion

In this letter, a deep learning-assisted demodulation methodology for THz wireless communication was proposed, which utilizes a multiple-output deep feedforward neural network to demodulate the received THz signals under hybrid distortions caused by the imperfections of THz devices. Specifically, a multiple-output deep feedforward neural network is trained to fit the mapping between received signal and likelihood information, where the number of outputs is equivalent to the size of the modulation set and the received THz signal is demodulated according to the likelihood information. Relying on the likelihood information, the overlapped received symbols corresponding to different constellation points could be demodulated reliably. In addition, a convenient training set generation method was proposed to generate the training examples without the prior knowledge of likelihood information. Simulation results demonstrated that our proposed demodulation methodology could improve the bit error rate performance considerably for THz receiver under severe hybrid distortions.

[9]LDPC in digital video broadcasting-second generation (DVB-S2) is utilized, where the number of bits in each LDPC block is 16200 [22].

References

[1] I. F. Akyildiz *et al.*, "TeraNets: Ultra-broadband communication networks in the terahertz band," *IEEE Wireless Commun.*, vol. 21, no. 4, pp. 130–135, Aug. 2014.

[2] K.-C. Huang and Z. Wang, "Terahertz terabit wireless communication," *IEEE Microw. Mag.*, vol. 12, no. 4, pp. 108–116, Jun. 2011.

[3] C. Han and Y. Chen, "Propagation modeling for wireless communications in the terahertz band," *IEEE Commun. Mag.*, vol. 56, no. 6, pp. 96–101, Jun. 2018.

[4] Z. Chen *et al.*, "A survey on terahertz communications," *China Commun.*, vol. 16, no. 2, pp. 1–35, Feb. 2019.

[5] B. Aazhang *et al.*, "Key drivers and research challenges for 6G ubiquitous wireless intelligence," Univ. Oulu, Oulu, Finland, White Paper, Sep. 2019. [Online]. Available: http://jultika.oulu.fi/files/isbn9789526223544.pdf

[6] Y. R. Ramadan *et al.*, "Precompensation and system parameters estimation for low-cost nonlinear tera-hertz transmitters in the presence of I/Q imbalance," *IEEE Access*, vol. 6, pp. 51814–51833, 2018.

[7] T. Schenk, *RF Imperfections in High-Rate Wireless Systems*. Amsterdam, The Netherlands: Springer, 2008.

[8] D. R. Morgan *et al.*, "A generalized memory polynomial model for digital predistortion of RF power amplifiers," *IEEE Trans. Signal Process.*, vol. 54, no. 10, pp. 3852–3860, Oct. 2006.

[9] M. Bozic and D. Budimir, "Joint compensation of I/Q impairments and power amplifier nonlinearity for concurrent dual-band transmitters using two-box model," *IEEE Microw. Wireless Compon. Lett.*, vol. 25, no. 5, pp. 340–342, May 2015.

[10] T. O'Shea and J. Hoydis, "An introduction to deep learning for the physical layer," *IEEE Trans. Cogn. Commun. Netw.*, vol. 3, no. 4, pp. 563–575, Dec. 2017.

[11] Y. Zhang *et al.*, "DeepWiPHY: Deep learning-based receiver design and dataset for IEEE 802.11ax systems," *IEEE Trans. Wireless Commun.*, vol. 20, no. 3, pp. 1596–1611, Mar. 2021.

[12] M. Honkala *et al.*, "DeepRx: Fully convolutional deep learning receiver," *IEEE Trans. Wireless Commun.*, vol. 20, no. 6, pp. 3925–3940, Jun. 2021.

[13] H. Wang *et al.*, "Deep learning for signal demodulation in physical layer wireless communications: Prototype platform, open dataset, and analytics," *IEEE Access*, vol. 7, pp. 30792–30801, 2019.

[14] K. Hornik *et al.*, "Multilayer feedforward networks are universal approximators," *Neural Netw.*, vol. 2, no. 5, pp. 359–366, Jan. 1989.

[15] S. Sharma and Y. Hong, "UWB receiver via deep learning in MUI and ISI scenarios," *IEEE Trans. Veh. Technol.*, vol. 69, no. 3, pp. 3496–3499, Mar. 2020.

[16] M. T. Hagan *et al.*, *Neural Network Design*. Boston, MA, USA: PWS, 1995.

[17] C. M. Bishop, *Neural Networks for Pattern Recognition*. Oxford, U.K.: Oxford Univ. Press, 1996.

[18] G. Colavolpe *et al.*, "Algorithms for iterative decoding in the presence of strong phase noise," *IEEE J. Sel. Areas Commun.*, vol. 23, no. 9, pp. 1748–1757, Sep. 2005.

[19] D. Li *et al.*, "Performance analysis of indoor THz communications with one-bit precoding," in *Proc. IEEE Global Commun. Conf. (GLOBECOM)*, Abu Dhabi, United Arab Emirates, Dec. 2018, pp. 1–7.

[20] N. Benvenuto and G. Cherubini, *Algorithms for Communications Systems and Their Applications*. Hoboken, NJ, USA: Wiley, 2002.

[21] S. R. Gunn, "Support vector machines for classification and regression," Image Speech Intell. Syst. Res. Group, Univ. Southampton, Southampton, U.K., Tech. Rep., 1997.

[22] *Digital Video Broadcasting (DVB); Second Generation Framing Structure, Channel Coding and Modulation Systems for Broadcasting, Interactive Services, New Gathering and Other Broadband Satellite Applications*, document EN ETSI 302 307 V1.4.1, 2014.